Alternatively Spliced Human TREK-1 Variants Alter TREK-1 Channel Function and Localization 1

Authors: Cowles, Chad L., Wu, Yi-Ying, Barnett, Scott D., Lee, Michael T., Burkin, Heather R., et al.

Source: Biology of Reproduction, 93(5)

Published By: Society for the Study of Reproduction

URL: https://doi.org/10.1095/biolreprod.115.129791

BIOLOGY OF REPRODUCTION (2015) **93**(5):122, 1–11
Published online before print 23 September 2015.
DOI 10.1095/biolreprod.115.129791

Alternatively Spliced Human TREK-1 Variants Alter TREK-1 Channel Function and Localization[1]

Chad L. Cowles, Yi-Ying Wu, Scott D. Barnett, Michael T. Lee, Heather R. Burkin, and Iain L.O. Buxton[2]

Myometrial Function Laboratory, Department of Pharmacology, University of Nevada School of Medicine, Reno, Nevada

ABSTRACT

TREK-1, an outward-rectifying potassium channel activated by stretch, is found in the myometrium of pregnant women. Decreased expression of TREK-1 near term suggests that TREK-1 may contribute to uterine quiescence during gestation. Five alternatively spliced TREK-1 variants were identified in the myometrium of mothers who delivered spontaneously preterm (<37 wk), leading to the hypothesis that these TREK-1 variants could interfere with TREK-1 function or expression. To investigate a potential role for these variants, immunofluorescence, cell surface assays, Western blots, and patch clamp were employed to study TREK-1 and TREK-1 variants expressed in HEK293T cells. The results of this study demonstrate that coexpression of TREK-1 with TREK-1 variants alters TREK-1 expression and suppresses channel function. Each variant affected TREK-1 in a disparate manner. In HEK293T cells coexpressing TREK-1 and each variant, TREK-1 membrane expression was diminished with compartmentalization inside the cell. When expressed alone, individual variants displayed channel properties that were significantly decreased compared to full-length TREK-1. In coexpression studies using patch clamp, basal TREK-1 currents were reduced by ~64% (4.3 vs. 12.0 pA/pF) on average at 0 mV when coexpressed with each variant. TREK-1 currents that were activated by intracellular acidosis were reduced an average of ~77% (21.4 vs. 94.5 pA/pF) at 0 mV when cells were transfected with TREK-1 and any one of the splice variants. These data correlate the presence of TREK-1 variants to reduced TREK-1 activity, suggesting a pathological role for TREK-1 variants in preterm labor.

electrophysiology, human myometrial smooth muscle, labor, myometrium, potassium channels, pregnancy, preterm labor, splice variants, TREK-1, uterus

INTRODUCTION

Recently, we described the gestational regulation of the two-pore domain, stretch-activated potassium channel (TREK-1) in human myometrium [1, 2]. Our group has previously shown that human TREK-1 transcripts, a product of gene KCNK2, are up-regulated in pregnant human myometrium and expression is decreased in term laboring tissues. This finding is consistent with a role for TREK-1 contributing to the maintenance of uterine quiescence by hyperpolarizing the cell membrane [3, 4]. A number of investigations have reported that TREK-1 is critical to physiological processes such as bio-electrogenesis, maintenance of vascular tone, and pain perception [5, 6]. Research has also suggested that improper TREK-1 function could be implicated in diseases of the central nervous system such as epilepsy. TREK-1 is different from some other K^+ channels because it requires a chemical or mechanical stimulus to be activated, unlike K^+ channels such as TASK-1 that remain open. It is therefore plausible that continuous stretching of the myometrium during gestation causes mechanical activation of TREK-1, contributing to uterine quiescence.

The majority of human genes have multi-exon subunits called variants that are generated by alternative splicing, a posttranscriptional mechanism that alters the pattern of gene expression, which increases the functional complexity of the human genome [7, 8]. Alternative splicing is important in cell regulation and physiological development, whereas aberrant splicing may be associated with cellular dysfunction and the clinical manifestation of disease [9, 10]. Alternative splice variants have been discovered for ion channels and receptor genes including P2X receptors, potassium channels, and calcium channels [11–16]. In our previous work we described five unique splice variants of TREK-1 in myometrial samples from mothers who delivered prematurely and confirmed that these variants physically interact with wild-type TREK-1 and alter cellular distribution [2].

TREK-1 splice variants have been identified in the brain, adrenal glands, and kidneys. One such splice variant, TREK-1Δex4, which was found in rat and mouse neurons, encodes a heavily truncated protein that consists of one transmembrane domain and one extracellular tail [17]. When TREK-1Δex4 was transiently transfected into HEK293 cells it was found to be nonconductive. When TREK-1 and TREK-1Δex4 were coexpressed in HEK293 cells, TREK-1Δex4 acted as an inhibitor of TREK-1 currents [17]. Another TREK-1 splice variant, TREK-1e, is generated when exon 5 is skipped and a frame shift in exon 6 occurs, causing termination of translation prematurely [18]. Similarly to TREK-1Δex4, TREK-1e demonstrated very little, if any, functional capacity, and, when coexpressed with TREK-1, decreased expression and TREK-1 currents. Descriptions of TREK-1 variants decreasing TREK-1 expression and activity confirm the importance of studying TREK-1 variants that have been discovered in the myometrium during pregnancy.

[1]Supported by grants to I.L.O.B. from the March of Dimes, Prematurity Initiative; National Institutes of Health grants R01 HD053028; U54GM104944; and a Gates Grand Challenges Grant. Institutional support was provided by NIH P20 RR016464 and the Mick Hitchcock, PhD Scholars Program.
[2]Correspondence: Iain L.O. Buxton, Foundation Professor & Chair, Pharmacology, 1664 N. Virginia Street, Reno, NV 89557-0318. E-mail: ibuxton@medicine.nevada.edu

Received: 17 April 2015.
First decision: 17 May 2015.
Accepted: 14 September 2015.

eISSN: 1529-7268 http://www.biolreprod.org
ISSN: 0006-3363

TABLE 1. Human uterine smooth muscle sample demographics.

Origin	Age (yr)	N	Diagnosis
TNL (38–41 wk)	22–41	7	CDMR[a] (5), preeclampsia (1), preeclampsia and gestational diabetes (1)
TL (39–40 wk)	27–35	6	Fetal indications[b] (4), bad tear (1), fetal distress (1)
PTNL (28–35 wk)	27–33	10	Fetal indications[c] (6), preeclampsia (2), previa bleeding (1), gestational diabetes with macrosomia (1)
PTL (26–37 wk)	20–39	9	PTL[c] (3), fetal indications[b] (4), elevated blood pressure (1), HELLP[d] syndrome (1)

[a] CDMR, elective cesarean delivery on maternal request.
[b] Postoperatively, fetal indications for C/S were listed.
[c] PTL was the only indication for C/S.
[d] Preeclampsia variant: Hemolysis, elevated liver enzymes and low platelet count.

MATERIALS AND METHODS

Human Uterine Smooth Muscle Tissue Collection

Term in-labor (TL), term nonlabor (TNL), preterm in-labor (PTL), and preterm nonlabor (PTNL) uterine tissues were collected with written informed consent. All research was reviewed and approved by the University of Nevada Biomedical Institutional Review Board (IRB) and the Renown Hospital IRB for the protection of human subjects. Myometrial biopsies were obtained from mothers undergoing cesarean section (C/S). Tissues were collected from patients in sPTL (gestational age 26–37 wk by ultrasound, singleton pregnancies) without infection based on the clinical indicators (patients with a high temperature and fever, rapid heartbeat, rapid fetal heartbeat, sweating, uterus tender to touch, or histological evidence of infection were not included as they might have had an infectious cause for their labor). Tissues were not collected if there was a vaginal discharge or any finding consistent with infection. The samples were taken from the superior aspect of the standard transverse incision. Women were sometimes in labor at the time of C/S as determined by the surgeon (contractions 2 min apart or less prior to surgery).

All clinical data on the treatments and the pregnancy course prior to C/S were collected without patient identifiers (Table 1). Exclusion criteria included age <21 yr; any infection, including vaginitis or suspected chorioamnionitis; use of oxytocin for labor induction; history of drug abuse; comorbid diagnoses such as HIV infection or AIDS; hepatitis C infection; uncontrolled diabetes; and any use of steroids, including topical use. Patients meeting our experimental criteria, which were established prior to this study, were consented by our laboratory manager after permission was received from the surgeon. The same criteria were used for nonlaboring patients, who were not experiencing regular contractions at a rate of <2 min. Our recent sample acquisition rates for term are 73% of requests, for TL 60%, and 40% and 35% for PTNL and sPTL respectively. There is currently no accepted measure of estimating gestational age and completely defining PTL timing [19]. For this reason, the cutoff gestation period for PTL and PTNL of 37 wk was used in this study [20]. Tissues were transported to the laboratory immediately in cold physiological buffer containing 120 mM NaCl, 5.0 mM KCl, 0.58 mM KH_2PO_4, 0.58 mM Na_2HPO_4, 2.5 mM $MgCl_2$, 20 mM α-D-glucose, 2.5 mM $CaCl_2$, 25 mM Tris, and 5.0 mM $NaHCO_3$; microdissected under magnification to isolate smooth muscle devoid of obvious blood vessels; snap frozen in liquid nitrogen; and stored at −150°C. The range of maternal and gestational ages and the reason for C/S delivery for patients contributing samples for this research are described in Table 1.

RNA Isolation and Quantitative Real-Time Polymerase Chain Reaction

Total RNA was isolated from 2–5 mg of frozen human myometrial homogenate using the MagMAX-96 Total RNA Isolation kit according to the manufacturer's protocol (Ambion, Austin, TX). DNA contamination was removed by treatment at room temperature with TURBO DNase. RNA was resuspended in 50 μl elution buffer provided with the kit.

First-strand complementary DNA was synthesized from 1 μg of total RNA using 250 ng random primers, 10 mM dNTPs, 10 mM dithiothreitol, and 200 U Superscript II reverse transcriptase (Invitrogen, Carlsbad, CA) at 37°C for 50 min and then inactivated at 70°C for 15 min. Ribonuclease H (2 units; Promega, Madison, WI) was employed to remove RNA at 37°C for 20 min. Before quantitative real-time PCR was performed, the specificity of each primer pair was monitored using Amplitag Gold Fast PCR Mix UP (2×; Applied Biosystems, Foster City, CA) in a 20-μl reaction volume.

PCR amplification was performed within the linear range using a Veriti 96 Well Fast Thermal Cycler (Applied Biosystems) adopting the first-strand cDNA from human uterine smooth muscle tissue bundles as the template under the following conditions: 95°C for 10 min as an initial melt, followed by 35 cycles at 96°C for 30 sec and annealing at 55°C for 30 sec, followed by a final extension at 72°C for 10 min. The cDNA of preterm myometrial tissue was used as the template. Equal amounts of PCR products were analyzed by gel electrophoresis and visualized using ethidium bromide staining. The primer sequences, annealing temperatures, and PCR product lengths are described in Table 2. Gene-specific primers for TREK-1 were designed from homologous areas of full-length TREK-1, including TREK-1 isoform A (NM_001017424.2; TREK-1a), TREK-1 isoform B (NM_014217.3; TREK-1b), and TREK-1 isoform C (NM_001017425.2; TREK-1c), using Integrated DNA Technologies Primer Quest software (Coralville, IA). Variant-specific primers were designed using Integrated DNA Technologies Primer Quest software. BLAST searches were performed to confirm that primer sequences were not homologous to any other known gene products, variants, or full-length TREK-1. Real-time PCR assays utilized Fast SYBR Green PCR Master Mix (Applied Biosystems) with ABI 7900 Real-Time PCR SDS software (Applied Biosystems) and experiments were carried out according to the manufacturer's instructions.

The reaction mixtures were composed of 1 μl primers (1 μM), 9 μl cDNA diluted in water, and 10 μl Fast SYBR Green PCR Master Mix (Applied Biosystems). Quantitative real-time PCR conditions were as follows: enzyme activation at 95°C for 20 sec; 40 cycles of denature at 95°C for 1 sec and anneal/extend at 60°C for 20 sec; and a single final dissociation step that

TABLE 2. Primer sequences, annealing temperatures, and PCR product lengths.

Primer	Direction	Sequence (5′→3′)	Tm (°C)[a]	Product length
TREK-1	Forward	GCCGCTCAGAACTCCAAACC	61.58	134
	Reverse	AGGACAACCACCAGGAATATCG	59.83	
SV-1	Forward	GATTTCTACTCAAATAGTGGCAGCA	59.41	109
	Reverse	GCCAGCAAAGAAGAAGGAACTTC	60.30	
SV-2	Forward	TCTACTGATTTGGAAACATCTCACC	58.83	194
	Reverse	AATCTTGGTCTGACTAACATTCCAC	59.06	
SV-3	Forward	ATTCCCCTCTTTGGTTTTCTCTTG	59.16	102
	Reverse	CGGATCCACAATAAACGTATCTTCC	59.82	
SV-4	Forward	GGGATTTCTACTGTGGATCCGAT	59.67	101
	Reverse	CAGGACAGCAGCAAAGTAAGCAA	61.05	
SV-5	Forward	CTACTGTGGGAGAGTTCAGAGC	59.83	140
	Reverse	CGAGAGCTTCCGCTTGATGG	61.15	
18S	Forward	CACGGCCGGTACAGTGAAA	60.30	72
	Reverse	AGAGGAGCGAGCGACCAA	60.68	

[a] Tm, melting temperature.

included 95°C for 15 sec, 60°C for 15 sec, and 95°C for 15 sec. Amplification of the transcript was measured by the fluorescence caused by SYBR Green binding to double-stranded DNA. Serial dilutions of cDNA were used for generating standard curves. The amount of specific target genes were calculated based on threshold cycle (Ct) values and extrapolating starting copy numbers from the standard curves. All samples were normalized to 18S rRNA amplification for controlling variation in sample quality.

Mutagenesis

The methods for TREK-1 cloning, the description of TREK-1 genetic splice variants, and the fact that TREK-1 and TREK-variants coimmunoprecipitate has been described [2]. Human influenza hemagglutinin (HA) epitope-tagged TREK-1 (HA-TREK-1) and 6xHis epitope-tagged splice variants (HSVs) were generated by deletion and insertion mutagenesis using the QuikChange II XL Site-Directed Mutagenesis Kit (Stratagene, La Jolla, CA). Epitope tagging of proteins using HA, HSV, and other recognition sequences is commonly used in similar studies of ion channels, including TREK-1, with no report of noticeable alterations in channel activity [18, 21]. TREK-1 cloned into the multiple-cloning site (MCS) of the pCDH-CMV-GFP+ Puro vector (GFP vector) and HA epitope (TACCCATACGATGTT-CCAGATTACGCA) were inserted into amino acid position 288 (pore 2-transmembrane 4 extracellular loop) of TREK-1 to generate a fusion construct containing the extracellular HA epitope [22]. Splice variants were cloned into the MCS of the pCDH-CMV-RFP vector (RFP vector) and the 6xHis epitopes (CACCACCACCACCACCAC) were inserted into the N-terminus of each TREK-1 splice variant to generate fusion constructs with an N-terminus of 6xHis epitope (HSV). The 5′ UTR and start codon of each splice variant were deleted and maintained in the same reading frame with a new start codon before the 6xHis sequence.

Cell Culture and Transfection

Human embryonic kidney cells containing the SV40 Large T-antigen (HEK293T) were maintained in a humidified 5% CO_2 and 95% O_2 incubator at 37°C with high-glucose growth medium (Dulbecco modified Eagle medium; Gibco BRL, Grand Island, NY) supplemented with 10% fetal bovine serum, 100 U/ml penicillin, and 100 μg/ml streptomycin. Cells were plated and maintained for transfection until 80% confluent. Cells were transfected with Lipofectamine 2000 (Invitrogen, Carlsbad, CA) using 6 μg plasmid DNA (1.0 μg of HA-TREK-1 and 5.0 μg of HSV) in 30-mm culture dishes. As a positive control (HA-TREK-1 only), pCDH-CMV-RFP vectors were cotransfected instead. Transfection efficiency ranged from ~60% to 70% for each DNA plasmid. Immunofluorescence studies with transfected cells were conducted after an incubation time of 48 h. For cell-surface assays and cell membrane separation, cells were transfected with Lipofectamine 2000 (Invitrogen) using 8 μg plasmid DNA (1.4 μg of HA-TREK-1 and 6.6 μg of HSV) for 100-mm^2 cell culture dishes. The pCDH-CMV-RFP was cotransfected with TREK-1 as a positive control, and the cells were ready for membrane TREK-1 detection or cell-surface assays after an incubation of 48 h.

Immunofluorescence

HA-TREK-1 and each HSV were premixed and transfected into HEK293T cells on coverslips in 30-mm^2 culture dishes using Lipofectamine 2000 and grown for 48 h. Transfected cells were fixed using 4% paraformaldehyde, permeabilized with 0.5% Triton X-100 for 5 min, and blocked for 1 h with 5% bovine serum albumin (BSA) in PBS (5% BSA/PBS). The primary antibody, HA-probe (F-7) mouse monoclonal anti-HA antibody (Santa Cruz Biotechnology Inc., Dallas, Texas), was diluted (1:50) in PBS containing 1% BSA and incubated for 1 h at room temperature; unbound primary antibodies were removed using three 10-min washes with PBS. Subsequently the secondary antibody, Alexa Fluor 405 Goat Anti-Mouse IgG (H+L; Life Technologies, Carlsbad, CA) was diluted (1:100) in 1% BSA/PBS and incubated with the sample for 1 h at room temperature; unbound secondary antibody was washed off using three 10-min washes. Coverslips were mounted using Vectashield Mounting Medium (Vector Laboratories, Burlingame, CA). Microscopy and data acquisition were carried out using an Olympus Fluoview FV1000 Confocal Microscope (Olympus, Shinjuku, Tokyo, Japan).

Cell-Surface Expression Assay and Membrane TREK-1 Detection

Transfected cells were used after an incubation of 48 h. Nonenzymatic cell dissociation solution (Sigma-Aldrich Co., St. Louis, MO) was applied to dissociate cells from dishes. For cell-surface assays, cells washed with PBS were blocked in 5% BSA/PBS for 1 h at 4°C. HA probes (F-7) were diluted in 1% BSA/PBS (1:200) and incubated for 1 h at 4°C. Afterwards, the cells were incubated with (1:1000) diluted horseradish peroxidase (HRP)-conjugated rabbit anti-mouse IgG (H+L) for 1 h at 4°C. After washing, 150 000 cells were diluted in 100 μl PBS and incubated with 100 μl of SIGMAFAST OPD (Sigma-Aldrich Co.) in the dark for 30 min with gentle shaking. TREK-1 on the cell surface was quantified using a colorimetric assay with a CHAMELEON V Plate reader (HIDEX, Turhu, Finland). HEK293T transfected with HA-TREK-1 was used as the positive control and different numbers of HA-labeled positive control cells were counted using a TC10 automated cell counter (Bio-Rad Laboratories, Hercules, CA) to generate a standard curve. The number of cells used to generate a standard curve ranged from 1×10^3 to 5×10^5. A Student *t*-test was used to compare HRP activity of HA-TREK-1 coexpressed with each variant to HA-TREK-1 coexpressed with RFP, which was used as the 100% activity control. Point-to-point statistical analysis was performed to compare the HRP activity of each variant coexpressed with TREK-1 to the activity of TREK-1 coexpressed with RFP.

For membrane TREK-1 detection, the transfected and dissociated cells were lysed in PBS with a sonicator, followed by 5 min of centrifugation at $9000 \times g$ to remove intracellular organelles. Cell membranes were collected by centrifugation at $100\,000 \times g$ for 2 h, followed by resuspension in lysis buffer that contained 190 mM NaCl, 50 mM Tris, 2% Triton X-100, 1% NP-40, 7 mM EDTA, and endogenous proteinase inhibitor cocktail (Thermo Fisher Scientific, Rockford, IL) with the pH adjusted to 7.4. Eluted protein (10 μg) was incubated at 95°C for 5 min with beta-mercaptoethanol and then subjected to SDS-PAGE for immunoblot analysis. Proteins were separated on 4%–20% precast polyacrylamide gels (Bio-Rad Laboratories) and transferred onto Trans-Blot Turbo Mini Nitrocellulose (Bio-Rad Laboratories). Detection was carried out using rabbit (H75) anti-TREK-1 antibodies at 1:1000 dilution (primary antibody) and incubated at 4°C for 12 h followed by washing and 1 h incubation with anti-rabbit 680 nm (secondary antibody) at 1:20 000 dilution at room temperature. This was followed by imaging on an Odyssey imaging system (LI-COR Biosciences, Lincoln, NE).

Electrophysiology

HEK293T cells were transfected using Lipofectamine 2000, 1 μg HA-TREK-1 plasmid, and 5 μg HSV plasmid for each of the TREK variants during coexpression experiments; 1 μg HA-TREK-1 or 5 μg of HSV plasmid was used for individual expression studies. The ratio of 1:5 was selected based on previous studies of TREK-1 variants that were discovered in other tissues that directly interacted with TREK-1. Overexpression of TREK-1 variants compared to wild-type TREK-1 has been utilized multiple times in the literature to gain an understanding of variant effects on channel activity [17, 18]. Successful transfection was verified using coexpression of fluorescent proteins in the plasmid DNA (green fluorescent protein with HA-TREK-1 and red fluorescent protein with each TREK-1 variant). Transfected cells were trypsin digested, plated on glass coverslips, and utilized for patch clamp experiments within 72 h of transfection. Transfected cells on glass coverslip shards were placed in a chamber mounted on top of an inverted microscope. The chamber was continuously perfused with a bath (external) solution that contained 140 mM NaCl, 5.4 mM KCl, 1.8 mM $CaCl_2$, 10 mM HEPES, 1 mM $MgCl_2$, 2 mM TEACl (to block voltage gated K^+ channels), 0.1 mM 4,4-diisothiocyanatostilbene-2,2-disulfonic acid (chloride channel blocker), and 0.1 mM $GdCl_3$ (nonspecific cation current blocker) with the pH adjusted to 7.4 and osmolarity adjusted to 310 mOsm/L with D-mannitol that was delivered by gravity through a manifold. Currents were recorded in the standard whole-cell variant of voltage clamp using pCLAMP software (V9.2; Axon Instruments/Molecular Devices Inc., Sunnyvale, CA). Pipettes were made of borosilicate glass (Sutter Instrument Co., Novato, CA) pulled on a two-stage vertical puller (pp-83; Narishige International US, Inc., East Meadow, NY) with a resistance of ~6 MΩ when filled with standard pipette solution. The pipette solution contained 140 mM KCl, 3 mM K_2ATP, 0.2 mM NaGTP, 5 mM HEPES, 1 mM $MgCl_2$, and 10 mM 1,2-bis(o-aminophenoxy)ethane-N,N,N′,N′-tetraacetic acid (to minimize Ca^{+2} activated K^+ currents) with the pH adjusted to 7.4 and osmolarity adjusted to 310 mOsm/L. Cell capacitance and series resistance were measured using the membrane test feature of pCLAMP and series resistance was compensated. Currents were amplified with an Axopatch200B amplifier (Axon Instruments/Molecular Devices Inc.) and digitized using a computer interfaced with a Digidata 1322A system (Axon Instruments/Molecular Devices Inc.). Currents were filtered at 1 kHz and digitized at 2 kHz for whole-cell recording. Whole-cell currents were normalized using cell capacitance to yield current density (pA/pF) for each cell. Whole-cell currents were monitored by running a pulse or ramp protocol every 15 sec stepping to +80 mV for 0.1 sec, ramping from +80 to −80 mV over 1 sec, and finally stepping to −80 mV for 0.1 sec. For all other whole-cell experiments, cells were held at 0 mV between pulse/ramp protocols. Currents were also observed using a step protocol during which they were held at 0 mV for 0.25 sec, an input

potential of −100 mV was applied for 0.5 sec, and the cells were held again for 0.25 sec at 0 mV; the potentials were increased by 20 mV for each recording until the input reached +100 mV. To elicit TREK-1 currents, a bath solution containing 90 mM sodium bicarbonate was perfused into the chamber, resulting in intracellular acidosis, a known activator of TREK-1 currents [23, 24]. Data were expressed as mean ± SEM. Student *t*-tests were used to compare mean values and paired tests were used when both conditions were measured on the same cell. *P* values less than 0.05 were deemed significant. A point-to-point analysis for each input voltage was utilized for statistical analysis to determine whether HA-TREK-1 and TREK-1 splice variant (HSV-1 through HSV-5) current changed after perfusion of $NaHCO_3$ into the bath solution and whether TREK-1 coexpressed with splice variants had a disparity in currents compared to RFP coexpressed with TREK-1 in NaCl or $NaHCO_3$ bath solutions.

RESULTS

Detection of TREK-1 and Splice Variants in Human Myometrium

TREK-1 is known to be present in human [2, 3]. TREK-1 mRNA transcript expression is up-regulated in TNL myometrium and significantly decreased in laboring and PTL tissues (Supplemental Fig. S1a; Supplemental Data are available online at www.biolreprod.org). In PTNL tissues (gestation age of 28–35 wk), the high expression of TREK-1 is consistent with the hypothesis that stretch activation of TREK-1 contributes to maintenance of uterine quiescence during gestation. Previously, we reported the discovery of five unique splice variants of human TREK-1 in preterm myometrium using RT-PCR. Variants are named SV-1 to SV-5 based on the number of exon deletions between exon 1 and 7 [3]. In this study, quantitative real-time PCR was utilized to investigate the expression of the five splice variants in different pregnancy states. Although TREK-1 and TREK-1 variants were not identified as up- or down-regulated during a recent RNAseq study, sequencing information and directed studies have shown TREK-1 and TREK-1 variant expression during all states of pregnancy, as seen in Supplemental Figure S1 [25]. It should be noted that although TREK-1 mRNA expression is relevant, oftentimes mRNA and protein abundance are present at levels that can vary more than 20-fold [26, 27].

We found that SV-1, SV-3, and SV-4 were highly expressed in TNL and PTNL samples (Supplemental Fig. S1, b, d, and e). The expression of SV-1 and SV-3 was higher in PTNL compared with TNL tissues. SV-2 expression in PTL was slightly higher than in TNL (Supplemental Fig. S1c). Interestingly, SV-5 was highly expressed in both PTL and PTNL tissues compared with TNL (Supplemental Fig. S1f).

TREK-1 Splice Variants Alter TREK-1 Expression in Transfected HEK293T Cells

In order to observe the interaction between each splice variant and TREK-1, each HSV in an RFP vector, referred to as HSV-1–HSV-5, and HA-tagged TREK-1 in a GFP vector (HA-TREK-1) were generated. The fluorescent proteins, RFP and GFP, were expressed bicistronically with the gene of interest and were used as indicators to verify successful transfection. Transfection efficiency was estimated by observing RFP or GFP in HEK293T cells. In general, ~60%–70% of cells expressed the fluorescent proteins, and this was consistent for HA-tagged TREK-1 and HSVs. TREK-1 expression was altered by coexpression of individual splice variants (Fig. 1). In order to eliminate any effect from cotransfection, HA-TREK-1 was cotransfected with an RFP vector as a control. The pattern of TREK-1 expression was different when TREK-1 was coexpressed with the variants compared with RFP-TREK-1. When TREK-1 was coexpressed with RFP, the majority of HA-tagged TREK-1 was located in the membrane. In the case of coexpression of each variant with TREK-1, localization of HA-tagged TREK-1 was predominately cytoplasmic. Subjectively, in cells that did not express the variant (as determined by lack of RFP), the expression of TREK-1 appears to be more membranous than in cells that heavily expressed splice variants (bright red cells). Coexpression of HSV-2, HSV-4, and HSV-5 appeared to reduce total TREK-1 expression; therefore, a cell surface assay was developed to more accurately quantify reductions in TREK-1 membrane expression.

TREK-1 Splice Variants Interfere with TREK-1 Trafficking to the Plasma Membrane

As a result of the discovery that individual variants altered TREK-1 expression by immunofluorescence, the role of TREK-1 variants on TREK-1 trafficking to the plasma membrane was investigated. HEK293T cells cotransfected with HA-TREK-1 and one of the variants were used without cellular permeabilization. Figure 2a shows a schematic of the TREK-1 cell surface expression assay. Reductions in membrane TREK-1 were observed (Fig. 2b), which indicates that splice variants are capable of reducing membrane TREK-1 expression, and could possibly interfere with TREK-1 trafficking and/or channel assembly. These results suggest that the presence of splice variants might alter TREK-1 channel activity and interfere with uterine quiescence. To further confirm the decrease in membrane TREK-1 expression and rule out a decrease in total TREK-1 expression, ultracentrifugation was used to separate membrane TREK-1 from cytosolic TREK-1 and fractions were analyzed using Western blot. Figure 2c depicts the detection of TREK-1 in membrane and cytosolic fractions in the presence or absence of HSV-1. Significantly more TREK-1 was expressed in the cytosolic fractions when TREK-1 was coexpressed with HSV-1. When TREK-1 was coexpressed with RFP as a control, TREK-1 was more abundant in the membrane fractions. These results confirmed that the presence of TREK-1 variants results in a reduction in functional TREK-1 expressed in the membrane. The data from this study demonstrated that compared to TREK-1 expressed with a plasmid control, TREK-1 expressed with SV-1 significantly reduced membrane expression. Therefore, it is plausible that TREK-1 trafficking to the membrane could be impacted by the presence of SV-1 or any of the other splice variants.

TREK-1 Splice Variants Demonstrate Limited Channel Activity

Patch clamp electrophysiology was used to further investigate functional properties of TREK-1 and individual splice variants. TREK-1 is an outwardly rectifying K^+ channel whose pharmacological profile is unique because it is insensitive to TEA, a classic antagonist of potassium channels, and can be activated by intracellular acidosis, a property that the other members of the TREK subfamily do not exhibit. In these experiments cells were allowed to establish a consistent basal current followed by exchanging the NaCl bath for 90 mM $NaHCO_3$ solution, which results in intracellular acidosis [24]. In the whole-cell patch clamp configuration, the currents from HEK293T cells transfected with each individual variant were explored. After current stabilization, a step protocol was used that applied potentials from −100 to +100 mV for 500 ms per voltage step in 20-mV intervals; cells were held at 0 mV for 250 ms between voltage steps. The currents from cells

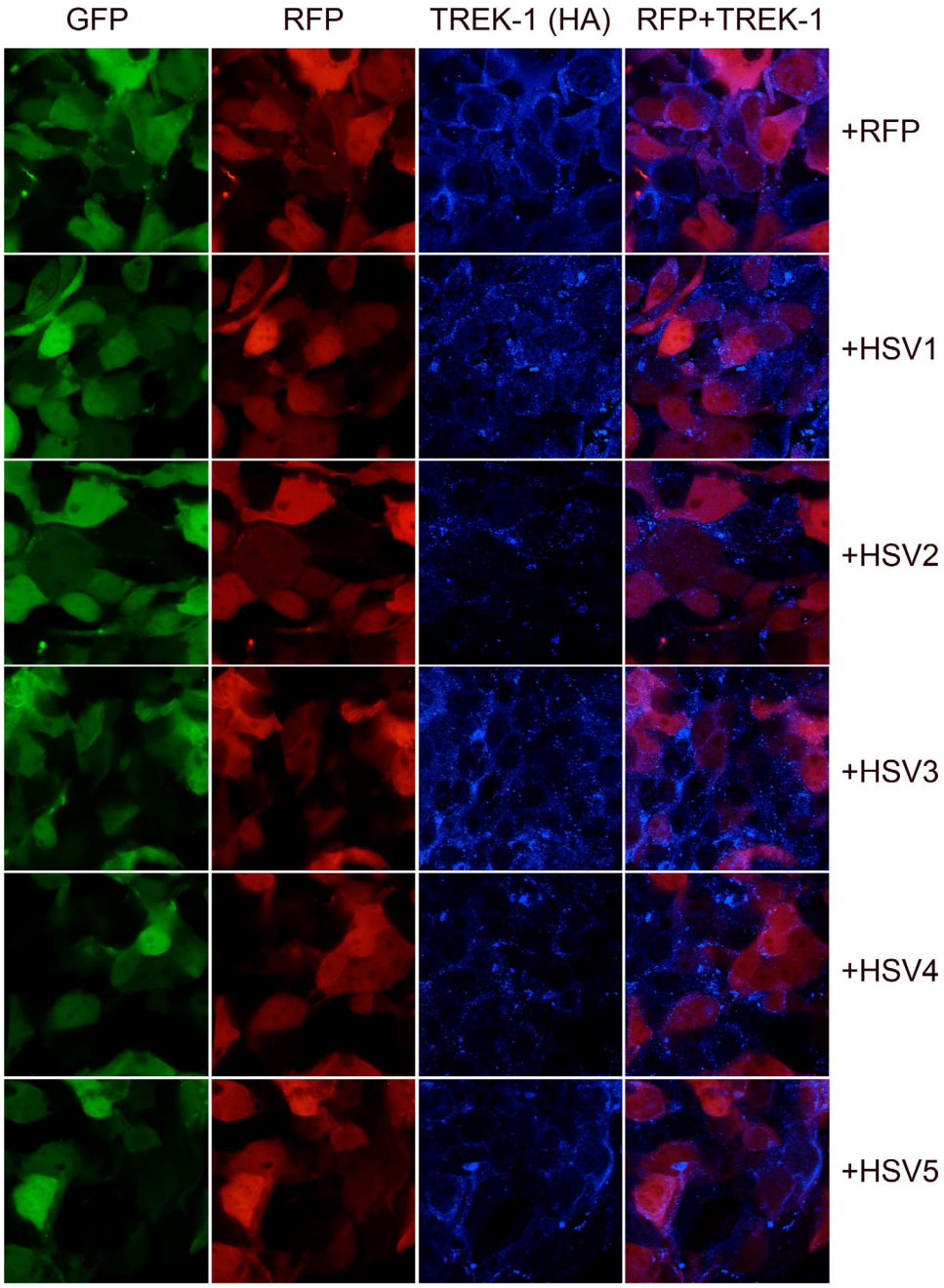

FIG. 1. Cellular localization of fluorescently labeled TREK-1 coexpressed with splice variants in HEK293T by confocal microscopy. HEK293 cells were transfected with HA-TREK-1 (1 μg) and each splice variant (5 μg). Cells were fixed, penetrated, and incubated with primary antibody (HA probe [F-7] mouse monoclonal anti-HA antibody) followed by incubation with secondary antibody Alexa Fluor 405 goat anti-mouse IgG. Micrographs show cellular localization of TREK-1 tagged with HA epitope (TREK-1) when TREK-1 is expressed with RFP or one of the variants. GFP indicates successful transfection of bicistronically expressed TREK-1 and GFP plasmid. RFP indicates successful transfection of bicistronically expressed HSV + RFP or RFP alone (5 μg). TREK-1 (HA) indicates detection of HA-tagged TREK-1 with mouse monoclonal anti-HA antibody. RFP + TREK-1 shows the overlay of cells expressing RFP + HSV plasmids and TREK-1 localization. Microscope settings for all images were as follows: eyepiece lens ×10; objective lens ×60; total magnification ×600; numerical aperture 1.42.

transfected with each variant alone as well as from TREK-1 expressed alone were measured (Fig. 3).

The basal current density for TREK-1 (5 μg; n = 7) at 0 mV was 14.7 ± 3.5 pA/pF; upon activation with 90 mM $NaHCO_3$, currents at 0 mV increased to 118.7 ± 14.3 pA/pF. The basal currents observed for each variant alone were 0.8 ± 0.06, 1.0 ± 0.06, 1.0 ± 0.04, 1.3 ± 0.09, and 0.8 ± 0.05 pA/pF for HSV-1 (n = 8), HSV-2 (n = 7), HSV-3 (n = 8), HSV-4 (n = 6), and HSV-5 (n = 7) at 0 mV, respectively. Upon perfusion of the bath with 90 mM $NaHCO_3$ at 0 mV the currents remained relatively unchanged at 0.91 ± 0.06, 0.84 ± 0.04, 1.49 ± 0.08, 1.82 ± 0.14, and 1.22 ± 0.12 pA/pF for HSV-1, HSV-2, HSV-3, HSV-4, and HSV-5, respectively. The average current and SEM for HA-TREK-1 and each variant expressed alone for each input voltage are shown in Supplemental Table S1. There was a slight, albeit significant, increase in current for HSV-3 upon $NaHCO_3$ perfusion into the bath solution. Nevertheless, for all other variants low basal channel activity was observed

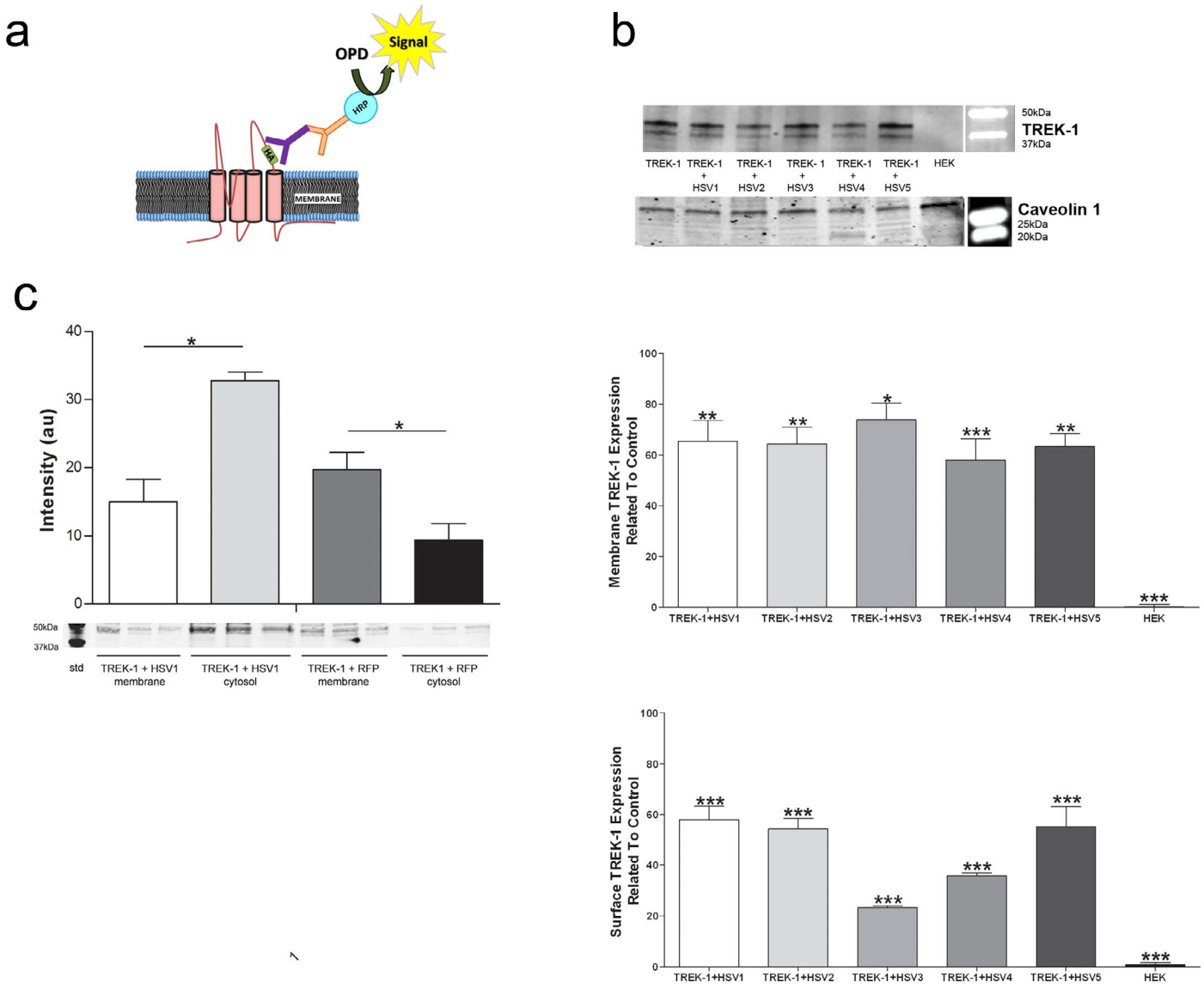

FIG. 2. Cell-surface and membrane TREK-1 expression. **a**) Schematic of HRP cell surface assay for detection of HA-TREK-1 in the membrane of transfected (1.0 μg of HA-TREK-1 and 5.0 μg of HSV) HEK293 cells without cellular permeabilization. HRP activity was used to quantify HA-TREK-1 on the cell surface after coexpression with each variant. Cell-surface TREK-1 was determined by HRP activity cotransfected with each individual HSV. Cells were incubated with HA probe (F-7) mouse monoclonal anti-HA antibody followed by incubation with HRP-conjugated rabbit anti-mouse IgG. HEK293T (nontransfected) cells were adopted as a negative control for specific measurement of extracellular HA. **b**) Top: Western blot data of membrane-bound TREK-1 expression (45 kDa) when TREK-1 is coexpressed with individual HSVs. Caveolin-1 (27 kDa) was adopted as an internal control for densitometric calculation. Western blot data were quantified from six such experiments. Bottom: Graphical representation of relative HRP activity for cells coexpressing TREK-1 and each variant compared to HA-TREK-1 (control) represented by 100%. $^{***}P < 0.005$; $^{**}P < 0.01$; $^{*}P < 0.05$. **c**) Western blot of membrane and cytosolic TREK-1 using fractionation assay. Cells were transfected with TREK-1 and RFP or HSV-1 (1.0 μg of HA-TREK-1 and 5.0 μg of HSV-1 or RFP) and lysed and membrane fractions were separated with 100 000 × *g* centrifugation for 2 h. Quantification was performed using densitometric calculation. $^{*}P < 0.05$.

(significantly different from TREK-1; data not shown) and little if any activation using intracellular acidosis ($NaHCO_3$ bath) could be discerned. Basal currents for TREK-1 and TREK-1 variants expressed alone compared with nontransfected HEK293 cells can be found in Supplemental Figure S2. Although the variants displayed low basal activity compared to TREK-1, higher currents were observed compared to nontransfected HEK293 cells. These data provide evidence that the currents detected for variants were minimal and could not be significantly increased using $NaHCO_3$, a well-established activator of TREK-1, indicating that the variants have little if any functional capacity.

TREK-1 Currents Are Inhibited in the Presence of Variants

Although TREK-1 splice variants were incapable of generating significant currents, their interaction with TREK-1 and the potential relationship to uterine quiescence was explored using cotransfection. Therefore, HEK293T cells were cotransfected with 1 μg TREK-1 and 5 μg of each splice variant; TREK-1 was also cotransfected with 5 μg RFP as an expression control. The average current-voltage relationships for basal (NaCl bath) TREK-1 currents in HEK293T cells cotransfected with TREK-1 and each of the variants compared to the basal current of TREK-1 cotransfected with RFP (the positive control) were observed (Fig. 4). When TREK-1 was

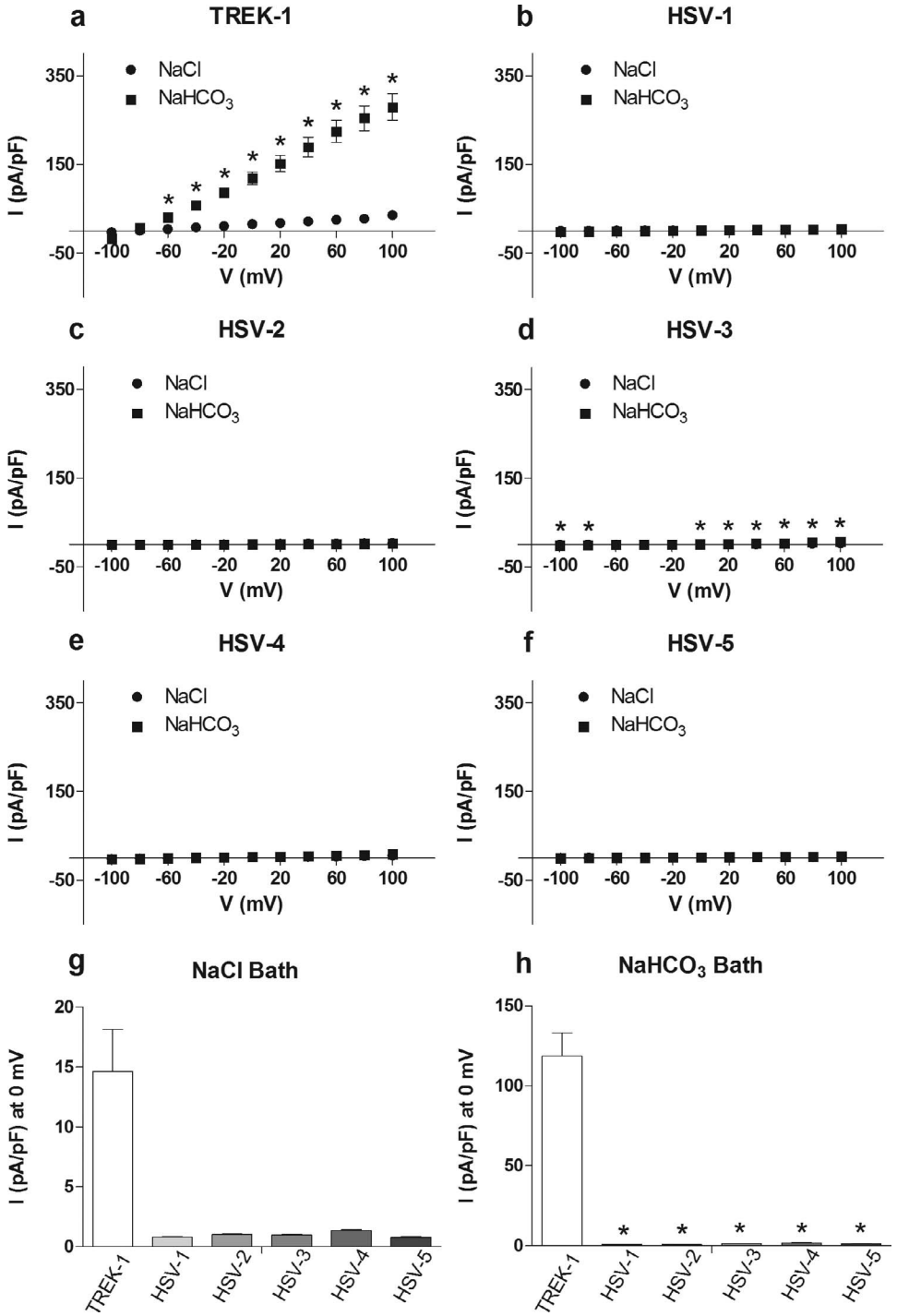

FIG. 3. Variants demonstrate low basal (NaCl) and $NaHCO_3$ currents. HEK293 cells on glass coverslips were transfected (1.0 μg of HA-TREK-1 or 5.0 μg of HSV) and placed in a recording chamber. Currents were recorded in the whole-cell mode of patch clamp. Currents were stabilized in an NaCl bath followed by perfusion of 90 mM $NaHCO_3$ into the bath solution. **a**–**f**) Mean whole-cell current densities in response to 20-mV voltage steps from −100 to +100 mV for HA-TREK-1 and each of the variants expressed alone in HEK293T cells before and after 90 mM $NaHCO_3$ perfusion into the external solution. TREK-1, n = 7; HSV-1, n = 8; HSV-2, n = 7; HSV-3, n = 8; HSV-4, n = 6; HSV-5, n = 7; *$P < 0.05$. **g**) Average currents at 0 mV in NaCl bath solution. **h**) Average currents at 0 mV in $NaHCO_3$ bath solution. *$P < 0.05$ between TREK-1 and variant currents.

cotransfected with the variants, the current was decreased; at 0 mV basal currents were 2.1 ± 0.6, 2.5 ± 0.1, 6.4 ± 0.3, 2.7 ± 0.2, and 7.5 ± 2.3 pA/pF for TREK-1 cotransfected with HSV-1 (n = 8), HSV-2 (n = 10), HSV-3 (n = 9), HSV-4 (n = 10), and HSV-5 (n = 8), respectively, compared to 11.97 ± 1.3 pA/pF for TREK-1 (n = 10) cotransfected with RFP. Supplemental Table S2 shows the average current and SEM for all of the tested voltages for TREK-1 cotransfected with each variant or RFP. This reduction in basal current was found to be significantly different for HSV-1, HSV-2, HSV-3, and HSV-4 at more positive (>40 mV) input potentials compared to TREK-1 coexpressing RFP. The relatively low basal current density observed was consistent with TREK-1 channel activity, which is reported to require a chemical or mechanical stimulus

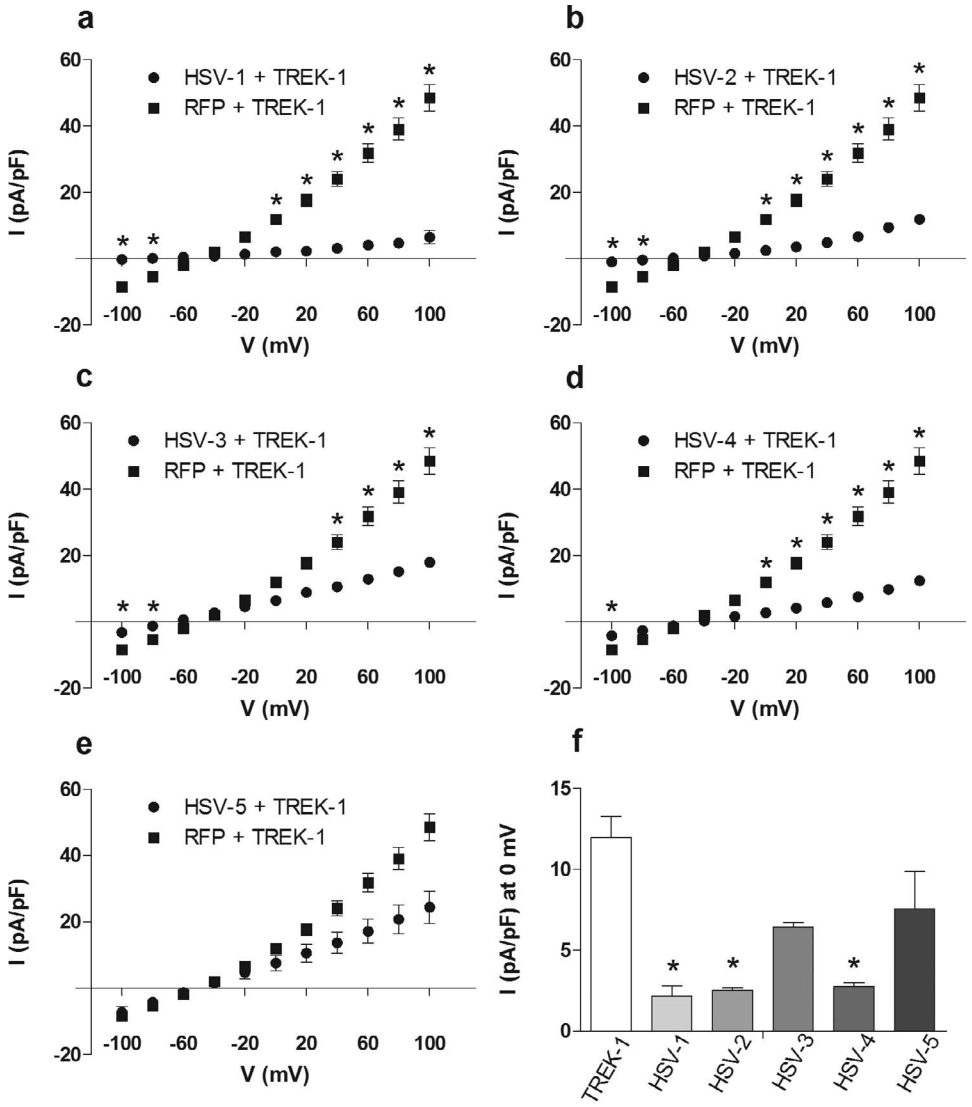

FIG. 4. Coexpression of wt-TREK-1 and TREK-1 splice variants decreases basal currents. HEK293 cells on glass coverslips were transfected (1.0 μg of HA-TREK-1 and 5.0 μg of HSV or RFP) and placed in a recording chamber. Currents were recorded in the whole-cell mode of patch clamp. Currents were stabilized in an NaCl bath for 2 min. **a**–**e**) Average mean whole-cell current densities in response to 20-mV steps from −100 to + 100 mV for TREK-1 coexpressing each individual splice variant compared with TREK-1 coexpressing RFP in standard 90 mM NaCl bath solution. TREK-1 + RFP, n = 10; TREK-1 + HSV-1, n = 8; TREK-1 + HSV-2, n = 10; TREK-1 + HSV-9, n = 8; TREK-1 + HSV-4, n = 10; TREK-1 + HSV-5, n = 8; $^*P < 0.05$ between average HA-TREK-1 + RFP current vs. TREK-1 HSV current. **f**) Average currents at 0 mV in NaCl bath solution for TREK-1 coexpressing RFP or each individual splice variant. $^*P < 0.05$.

to open. To test if activated TREK-1 currents were altered in the presence of variants after the basal currents were stabilized, $NaHCO_3$ was perfused in the bath solution. In general, depending on the exact perfusion rate, currents would increase within 3–5 min and would stabilize after 5–7 min. Figure 5 shows the activated currents for TREK-1 coexpressing each of the variants compared to TREK-1 coexpressing RFP. The average currents at 0 mV were 20.7 ± 5.8, 19.7 ± 2.1, 26.0 ± 2.9, 24.4 ± 2.7, and 16.3 ± 3.8 pA/pF for HSV-1, HSV-2, HSV-3, HSV-4, and HSV-5, respectively, compared to the significantly higher activation of 94.5 ± 8.9 pA/pF for TREK-1 coexpressing RFP. When applied voltages were −40 mV or greater, there was a significant difference between TREK-1-coexpressing variants compared to coexpression with RFP. The average currents and SEM of TREK-1 coexpressing each of the variants or RFP at every input potential are shown in Supplemental Table S3. These data show that activated TREK-1 currents are decreased in the presence of each of the splice variants. It should be pointed out that compared to variants expressed alone, HSV-2, HSV-3, HSV-4, and HSV-5 coexpressed with TREK-1 demonstrated activation that was significantly greater (Supplemental Fig. S3). These activated currents most likely are generated by TREK-1 that is expressed and still functional. Collectively, the functional assessment of TREK-1 and TREK-1 splice variants indicates that 1) variants demonstrate minimal currents and show little if any activation by intracellular acidosis, 2) TREK-1 basal currents are generally decreased when splice variants are coexpressed (~64% average reduction), and 3) activated TREK-1 currents are more significantly decreased than basal currents when splice variants are coexpressed (~77% average reduction).

DISCUSSION

We previously identified TREK-1 in pregnant human myometrium, leading to the hypothesis that TREK-1 activity

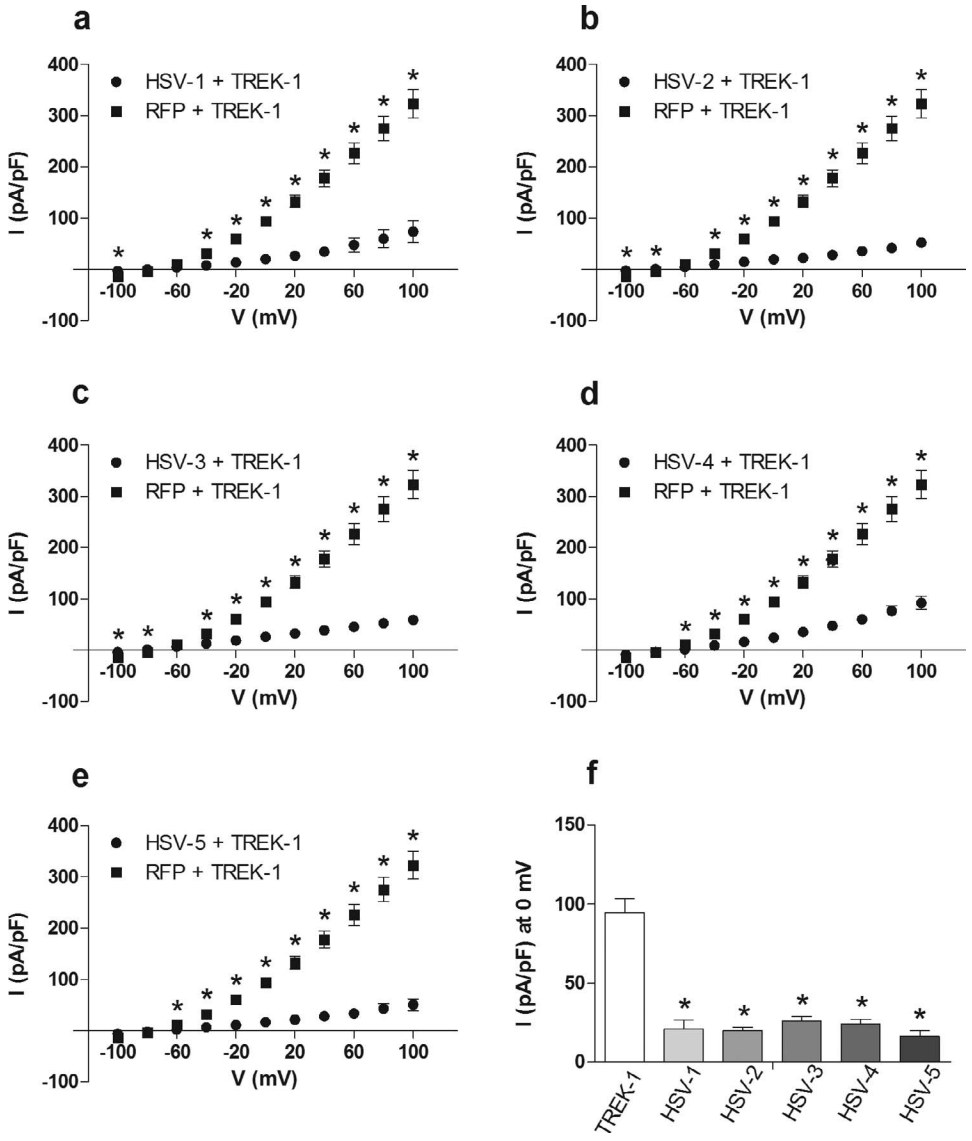

FIG. 5. Coexpression of wt-TREK-1 with TREK-1 splice variants decreases activated currents. HEK293 cells on glass coverslips were transfected (1.0 μg of HA-TREK-1 and 5.0 μg of HSV or RFP) and placed in a recording chamber. Currents were recorded in the whole-cell mode of patch clamp. Currents were stabilized in an NaCl bath followed by perfusion of $NaHCO_3$ into the chamber; activated currents were stabilized for 2 min. **a**–**e**) Average mean whole-cell current densities in response to 20 mV steps from −100 to +100 mV for HA-TREK-1 coexpressing each individual splice variant compared with HA-TREK-1 coexpressing RFP in standard 90 mM NaCl bath solution. TREK-1 + RFP, n = 10; TREK-1 + HSV-1, n = 8; TREK-1+ HSV-2, n = 10; TREK-1 + HSV-9, n = 8; TREK-1 + HSV-4, n = 10; TREK-1 + HSV-5, n = 8; $^*P < 0.05$ between average HA-TREK-1 + RFP current vs. TREK-1 HSV current. **f**) Average currents at 0 mV in $NaHCO_3$ bath solution for TREK-1 coexpressing RFP or each individual splice variant. $^*P < 0.05$.

contributes to the maintenance of uterine quiescence during gestation toward term, and suspected that decreased TREK-1 expression could coincide with premature labor [4]. In preterm human myometrium, splice variants of TREK-1 (SV-1–SV-5) were discovered [2]. In this study, the effects of splice variants on TREK-1 were characterized in detail in a model cell system. In pregnant nonlaboring human myometrium TREK-1 transcripts were determined to be up-regulated, but at the onset of labor TREK-1 was down-regulated. The relatively high expression in PTNL and decreased expression in TNL myometrium suggest that TREK-1 is involved in maintaining uterine quiescence before 37 wk of human gestation. The dramatic decrease in TREK-1 expression observed in TL patients supports this hypothesis. The transcripts for each of the five TREK-1 variants were discovered to be present in each pregnancy phase (TNL, TL, PTL, and PTNL) at disparate levels. However, the presence of the splice variant transcripts does not necessarily correlate to protein expression [26, 27] and so the impact of these variants on TREK-1 was further studied.

The interactions between TREK-1 and each individual variant were studied using immunofluorescence, cell surface assays, Western blots, and electrophysiology. The results from each of these studies demonstrated that TREK-1 expression and function were significantly altered and/or reduced compared to TREK-1 transfected with a plasmid control when coexpressed in a model cell system. These data indicate that each of the five TREK-1 splice variants has a dominant inhibitory effect on TREK-1.

In the overexpressed system, the observed abatement of TREK-1 protein and its altered cellular distribution by individual variants provide evidence that splice variants compete with TREK-1 for translation factors. Even though the mechanism of TREK-1 protein synthesis was not studied,

the general mechanism of protein synthesis begins with the initiation of binding at an *AUG* start codon. Taken together, these unique myometrial splice variants of TREK-1 might compete with TREK-1 for translation factors, which results in TREK-1 expression reduction in HEK293T cells because the start codon at the 5′ location is conserved between variants and TREK-1 based on nucleotide sequences [2]. The microtubule-associated protein Mtap2 binds to microtubules and stabilizes the microtubule network. Mtap2 has been shown to increase mouse TREK-1 current density at the plasma membrane by binding to amino acids at a central C-terminus (YDKF QRATSIKRKLSAELAGNHNQ), which is conserved between humans and mice [28]. These amino acids are conserved in SV-2 and SV-4, which could explain the reduction of TREK-1 currents in the presence of variants SV-2 or SV-4. Furthermore, the N-terminus of rat TREK-1 was found to be essential for enhancing TREK-1 trafficking to the plasma membrane by direct interaction with β-COP, a subunit of coat protein complex 1 [22]. Considering that all of the variants studied retain partial N-termini, the decreased expression of membrane TREK-1 could be explained through the utilization of β-COP from TREK-1 forward trafficking resulting in lower membrane TREK-1 expression. Premature truncation as a result of exon skipping has been reported to produce nonfunctional potassium channels [17]. TREK-1 currents were reduced by all of the variants. Although the mechanism causing decreased basal currents has yet to be elucidated, the dominant negative effects of splice variants have also been observed in rat TREK-1 channels and other ion channels [17, 29, 30].

Intracellular acidification has been shown to reduce the frequency of uterine contractions in humans and rats [31]. Intracellular pH has been shown to alter contractions in skeletal muscle as well as smooth muscle, but with variable effects based on the type of muscle. In rat myometrium, intracellular acidification inhibits contractions [31]. Acidification of the myometrial membrane during gestation may activate TREK-1 channel activity because intracellular acidification is one of the known activators of TREK-1 [3, 23]. In humans, alkalinization of intracellular uterine pH over the last few weeks of gestation has been hypothesized to contribute to contractions during labor [31]. The charged cluster in the proximal C-terminus D294-E309 (DWLRVISKKTK-EEVGE) has been reported to be critical for TREK-1 activation [24, 32, 33]. The specific glutamate residue (E306) is the intracellular proton sensor for channel activation by intracellular acidosis [34]. TREK-1 currents were reduced by an average of ~77% after exchanging $NaHCO_3$ into the bath solution to cause intracellular acidosis when TREK-1 was coexpressed with each variant. Our data suggest that the residual currents were generated by the TREK-1 channels that avoided variant mediated inhibition. It is possible that the greater reduction in $NaHCO_3$-activated currents compared to basal currents (~64% on average) in the presence of variants is a result of competitive protonation of variants rather than TREK-1.

It is also possible that splice variants play dominant effects on reducing TREK-1 expression by competing for translation factors, which reduces membrane TREK-1 expression and current densities by utilizing carrier proteins of forward trafficking. Furthermore, variants could assemble with TREK-1 as heterodimers, which form nonfunctional multiplex TREK-1 channels. The dominant negative effects of a nonconducting TREK-1 splice variant that was discovered in mouse brain that consisted of a homologous N-terminus, transmembrane segment 1, and a small part of pore loop 1 retained TREK-1 inside the cells and reduced TREK-1 currents. The N-terminus of TREK-1 is required for this assembly [17]. HIV-1 accessory protein Vpu, which contains a transmembrane domain, assembles with the first transmembrane segment of TASK-1, resulting in the abolishment of TASK-1 currents [35]. In accordance with this, the dominant effects on TREK-1 may be due to the direct or indirect interaction between the N-terminus of TREK-1 and the partial N-terminus of splice variants. SV-1 possesses a partial N-terminus that is followed by a transmembrane domain. The predicted structure of SV-1 is similar to that of the variant that was discovered in the mouse brain that was found to assemble with TREK-1. SV-4 retains a partial N-terminus that is followed by homologs of transmembrane segment 4 and the C-terminus and could assemble with TREK-1. The presence of transmembrane segment 4 and the C-terminus may directly or indirectly change the conformation of TREK-1 and reduce channel activity. These partial residues (MMNPRAKRDFY) of the N-terminus from SV-2, SV-3 and SV-5 may assemble heterogeneously with TREK-1 and change the three-dimensional conformation of TREK-1.

These studies provide compelling insights into the interaction between TREK-1 and TREK-1 splice variants, which could be related to various pathological conditions including PTL. Although these specific investigations were performed in a model cell system, future studies will focus on these interactions in specific patient samples. By determining that TREK-1 activity is substantially impacted by the presence of splice variants and TREK-1 expression is gestationally regulated, new insight into uterine physiology during pregnancy is gained. It is quite plausible that future research will discover that specific patients who express TREK-1 variants also exhibit decreased TREK-1 activity. If TREK-1 activity is decreased, a patient could be more likely to experience uterine quiescence failure and have an increased chance of delivering prematurely.

The individual interaction of each variant with TREK-1 needs to be further investigated, and it is possible that each hypothesized inhibition mechanism—variant protonation, translation factor competition, or heterodimer formation—acts individually or in concert to decrease TREK-1 expression and channel activity. Although the ability of TREK-1 variants to alter stretch-activated channel availability in the membrane as well as channel function is an important observation, it does not directly clarify the expression levels seen in patients. It is not clear why we see reduced levels of SV1-4 in PTL versus PTNL. To extend this work, a range of transfection ratios will be studied, including transfection of ratios that most closely represent those observed in different pregnancy stages, to develop a better understanding of conditions that are directly physiologically relevant. This may be complicated by events at the time of labor that are unknown. Nonetheless, the fact that expression of variants in the HEK cell system suppresses TREK-1 currents may be indicative of their contribution to PTL mechanisms in women. Our data suggest that comprehensive studies should be performed to correlate TREK-1 activity with uterine quiescence during pregnancy.

ACKNOWLEDGMENT

The authors acknowledge the Renown Hospital Medical Center for their assistance in this work. We thank Sara Thompson, RN, for expert assistance as a clinical coordinator.

REFERENCES

1. Heyman NS, Cowles CL, Barnett SD, Wu YY, Cullison C, Singer CA, Leblanc N, Buxton IL. TREK-1 currents in smooth muscle cells from

pregnant human myometrium. Am J Physiol Cell Physiol 2013; 305: C632–C642.
2. Wu YY, Singer CA, Buxton IL. Variants of stretch-activated two-pore potassium channel TREK-1 associated with preterm labor in humans. Biol Reprod 2012; 87:96.
3. Buxton ILO, Heyman N, Wu Y-YY, Barnett S, Ulrich C. A role of stretch-activated potassium currents in the regulation of uterine smooth muscle contraction. Acta Pharmacol Sin 2011; 32:758–764.
4. Tichenor JN, Hansen ET, Buxton IL. Expression of stretch-activated potassium channels in human myometrium. Proc West Pharmacol Soc 2005; 48:44–48.
5. Mongahan K, Baker SA, Dwyer L, Hatton WC, Park KS, Sanders KM, Koh SD. The stretch-dependent potassium channel TREK-1 and its function in murine myometrium. J Physiol 2011; 589:1221–1233.
6. Alloui A, Zimmermann K, Mamet J, Duprat F, Noel J, Chemin J, Guy N, Blondeau N, Voilley N, Rubat-Coudert C, Borsotto M, Romey G, et al. TREK-1, a K+ channel involved in polymodal pain perception. EMBO J 2006; 25:2368–2376.
7. Modrek B, Lee C. A genomic view of alternative splicing. Nat Genet 2002; 30:13–19.
8. Pan Q, Shai O, Lee LJ, Frey BJ, Blencowe BJ. Deep surveying of alternative splicing complexity in the human transcriptome by high-throughput sequencing. Nat Genet 2008; 40:1413–1415.
9. Pedrotti S, Bielli P, Paronetto MP, Ciccosanti F, Fimia GM, Stamm S, Manley JL, Sette C. The splicing regulator Sam68 binds to a novel exonic splicing silencer and functions in SMN2 alternative splicing in spinal muscular atrophy. EMBO J 2010; 29:1235–1247.
10. Gao G, SC. Jr. Dudley RBM25/LUC7L3 function in cardiac sodium channel splicing regulation of human heart failure. Trends Cardiovasc Med 2013; 23:5–8.
11. Koshimizu TA, Kretschmannova K, He ML, Ueno S, Tanoue A, Yanagihara N, Stojilkovic SS, Tsujimoto G. Carboxyl-terminal splicing enhances physical interactions between the cytoplasmic tails of purinergic P2X receptors. Mol Pharmacol 2006; 69:1588–1598.
12. Chen L, Tian L, MacDonald SH, McClafferty H, Hammond MS, Huibant JM, Ruth P, Knaus HG, Shipston MJ. Functionally diverse complement of large conductance calcium- and voltage-activated potassium channel (BK) alpha-subunits generated from a single site of splicing. J Biol Chem 2005; 280:33599–33609.
13. Ohya S, Sergeant GP, Greenwood IA, Horowitz B. Molecular variants of KCNQ channels expressed in murine portal vein myocytes: a role in delayed rectifier current. Circ Res 2003; 92:1016–1023.
14. Chaudhuri D, Chang SY, DeMaria CD, Alvania RS, Soong TW, Yue DT. Alternative splicing as a molecular switch for Ca2+/calmodulin-dependent facilitation of P/Q-type Ca2+ channels. J Neurosci 2004; 24:6334–6342.
15. Krovetz HS, Helton TD, Crews AL, Horne WA. C-terminal alternative splicing changes the gating properties of a human spinal cord calcium channel alpha 1A subunit. J Neurosci 2000; 20:7564–7570.
16. Zhuchenko O, Bailey J, Bonnen P, Ashizawa T, Stockton DW, Amos C, Dobyns WB, Subramony SH, Zoghbi HY, Lee CC. Autosomal dominant cerebellar ataxia (SCA6) associated with small polyglutamine expansions in the alpha 1A-voltage-dependent calcium channel. Nat Genet 1997; 15: 62–69.
17. Veale EL, Rees KA, Mathie A, Trapp S. Dominant negative effects of a non-conducting TREK1 splice variant expressed in brain. J Biol Chem 2010; 285:29295–29304.
18. Rinné S, Renigunta V, Schlichthörl G, Zuzarte M, Bittner S, Meuth SG, Decher N, Daut J, Preisig-Müller R. A splice variant of the two-pore domain potassium channel TREK-1 with only one pore domain reduces the surface expression of full-length TREK-1 channels. Pflugers Arch Eur J Physiol 2014; 466:1559–1570.
19. Kramer MS, Papageorghiou A, Culhane J, Bhutta Z, Goldenberg RL, Gravett M, Iams JD, Conde-Agudelo A, Waller S, Barros F, Knight H, Villar J. Challenges in defining and classifying the preterm birth syndrome. Am J Obstet Gynecol 2012; 206:108–112.
20. Goldenberg RL, Culhane JF, Iams JD, Romero R. Epidemiology and causes of preterm birth. Lancet 2008; 371:75–84.
21. Watschinger K, Horak SB, Schulze K, Obermair GJ, Wild C, Koschak A, Tampé R, Striessnig J. Functional properties and modulation of extracellular epitope-tagged Ca V 2. 1 voltage-gated calcium. Channels (Austin) 2008; 2:461–473.
22. Kim E, Hwang EM, Yarishkin O, Yoo JC, Kim D, Park N, Cho M, Lee YS, Sun CH, Yi GS, Yoo J, Kang D, et al. Enhancement of TREK1 channel surface expression by protein-protein interaction with beta-COP. Biochem Biophys Res Commun 2010; 395:244–250.
23. Bai X, Bugg GJ, Greenwood SL, Glazier JD, Sibley CP, Baker PN, Taggart MJ, Fyfe GK. Expression of TASK and TREK, two-pore domain K+ channels, in human myometrium. Reproduction 2005; 129:525–530.
24. Maingret F, Patel AJ, Lesage F, Lazdunski M, Honore E. Mechano- or acid stimulation, two interactive modes of activation of the TREK-1 potassium channel. J Biol Chem 1999; 274:26691–26696.
25. Chan Y-W, van den Berg HA, Moore JD, Quenby S, Blanks AM. Assessment of myometrial transcriptome changes associated with spontaneous human labour by high-throughput RNA-seq. Exp Physiol 2014; 99:510–524.
26. Gygi SP, Rochon Y, Franza BR, Aebersold R. Correlation between protein and mRNA abundance in yeast. Mol Cell Biol 1999; 19:1720–1730.
27. Greenbaum D, Colangelo C, Williams K, Gerstein M. Comparing protein abundance and mRNA expression levels on a genomic scale. Genome Biol 2003; 4:117.
28. Sandoz G, Tardy MP, Thummler S, Feliciangeli S, Lazdunski M, Lesage F. Mtap2 is a constituent of the protein network that regulates twik-related K+ channel expression and trafficking. J Neurosci 2008; 28:8545–8552.
29. Makielski JC, Ye B, Valdivia CR, Pagel MD, Pu J, Tester DJ, Ackerman MJ. A ubiquitous splice variant and a common polymorphism affect heterologous expression of recombinant human SCN5A heart sodium channels. Circ Res 2003; 93:821–828.
30. Shang LL, Pfahnl AE, Sanyal S, Jiao Z, Allen J, Banach K, Fahrenbach J, Weiss D, Taylor WR, Zafari AM, Dudley SC Jr. Human heart failure is associated with abnormal C-terminal splicing variants in the cardiac sodium channel. Circ Res 2007; 101:1146–1154.
31. Taggart M, Wray S. Simultaneous measurement of intracellular pH and contraction in uterine smooth muscle. Pflugers Arch 1993; 423:527–529.
32. Maingret F, Patel AJ, Lesage F, Lazdunski M, Honore E. Lysophospholipids open the two-pore domain mechano-gated K(+) channels TREK-1 and TRAAK. J Biol Chem 2000; 275:10128–10133.
33. Patel AJ, Honore E, Maingret F, Lesage F, Fink M, Duprat F, Lazdunski M. A mammalian two pore domain mechano-gated S-like K+ channel. EMBO J 1998; 17:4283–4290.
34. Patel AJ, Honore E. 2P domain K+ channels: novel pharmacological targets for volatile general anesthetics. Adv Exp Med Biol 2003; 536: 9–23.
35. Hussain A, Wesley C, Khalid M, Chaudhry A, Jameel S. Human immunodeficiency virus type 1 Vpu protein interacts with CD74 and modulates major histocompatibility complex class II presentation. J Virol 2008; 82:893–902.